

Atomic interference phenomena in solids with a long-lived spin coherenceElena Kuznetsova,^{1,2,*} Olga Kocharovskaya,^{1,2} Philip Hemmer,³ and Marlan O. Scully^{1,3,4}¹*Department of Physics, Texas A&M University, College Station, Texas 77843-4242*²*Institute of Applied Physics RAS, 46 Ulyanov Str., Nizhny Novgorod, 603600, Russia*³*Department of Electrical Engineering, Texas A&M University, College Station, Texas 77843*⁴*Max-Planck-Institut für Quantenoptik, D-85748 Garching, Germany*

(Received 07 May 2002; published 6 December 2002)

We generalize the theory of electromagnetically induced transparency (EIT) and slow group velocity for the case of the homogeneous and inhomogeneous line broadening in both one- and two-photon transitions which unavoidably takes place in solid materials with a long-lived spin coherence. We identify regimes of EIT where the linewidth can be essentially reduced due to inhomogeneous broadening and, moreover, can be proportional to the amplitude of the driving field rather than the intensity. We suggest also a class of solid materials, namely, rare-earth ion doped semiconductors or dielectrics with electricdipole allowed transitions, that is very promising for realization and applications of EIT.

DOI: 10.1103/PhysRevA.66.063802

PACS number(s): 42.50.Gy, 42.50.Ct

I. INTRODUCTION

Electromagnetically induced transparency (EIT) is the optical transparency of a three-level medium at a resonant transition induced by application of a coherent electromagnetic field at an adjacent transition. The accompanying reduction of the group velocity of light by orders of magnitude in the EIT transparency window has been intensively studied [1–3] in connection with many potential applications, especially low-intensity nonlinear optics [4,5] and quantum information storage and processing [6,7]. Most of the theoretical and experimental work so far (with the exception of a few recent experiments [8–11]) has dealt with gaseous media. Motivated by practical considerations, to implement (EIT) in real devices one turns to solid materials. Indeed, the obvious advantages of solids are high density of atoms, compactness, absence of atomic diffusion (which is especially important for optical memory), and simplicity and convenience in preparation and usage. On the other hand, the commonly known difficulties with realization of atomic interference effects in solids are typically very broad optical lines and fast decay of any coherence.

At the moment a few pioneering proof-of-principle EIT experiments have been performed in three different types of solid materials: rare-earth ion doped crystals with forbidden transitions lying in the band gap of a crystal [8], $N-V$ centers in diamond [9–11], and quantum wells in semiconductors [12,13]. Transparency of the order of 100% was achieved in some of them [8–11]. However, this required much higher intensities than in gaseous media and resulted in larger EIT linewidths. The obvious difficulty of dealing with semiconductors is the very fast decay (picoseconds) of electronic coherence. On the other hand, the spin coherence decay time in EIT experiments [8,11] is of the same order of magnitude (tens or hundreds of microseconds) as in experiments with gases [14,15].

Several questions arise. (i) What is the threshold for the

driving field providing EIT in solid materials? (ii) What is the EIT linewidth dependence on the intensity of the driving field and other parameters of the system? (iii) What determines the efficiency of nonlinear transformations and quantum light storage in solids? In order to answer these questions, to explain the recent experimental data [8,11,14,23,25,26], and to identify the optimal regimes and the most suitable materials for realization of EIT, we here generalize the theory of EIT for the case of solids with long-lived coherence. We take into account the major specifics of these materials as compared to gaseous media, namely, homogeneous and inhomogeneous line broadening of both optical and spin transitions as well as the difference between the longitudinal T_1 (spin-lattice) and transverse T_2 (spin-spin) relaxation times in a low-frequency transition. In gases T_1 and T_2 are typically indistinguishable, being defined by the lifetime of the atoms in the light beam.

The paper is organized as follows. In Sec. II we derive general density matrix equations governing the evolution of a Λ system, necessary for calculation of the macroscopic polarization of a medium. In Sec. III we derive the linewidth of EIT resonance. In Sec. IV we study the group velocity in the vicinity of the EIT resonance. In Sec. V we analyze recent experimental observations of EIT in solids [8,11]. In Sec. VI we discuss the major material requirements and suggest a class of promising solid media for EIT and slow group velocity (SGV) related experiments. In the Appendix we describe the procedure for determining the polarization averaged over the inhomogeneous profiles.

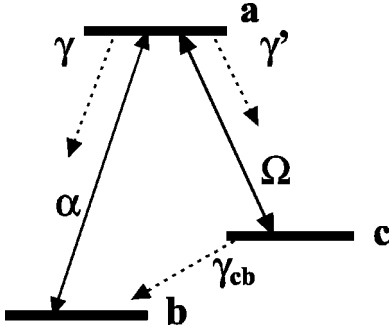
II. SUSCEPTIBILITY OF A Λ SYSTEM

Let us consider the energy scheme depicted in Fig. 1. In this three-level Λ scheme one of the two lower levels (c) is coupled to the upper level (a) by a coherent drive laser and the transition $a \rightarrow b$ is probed by a weak coherent field. The atomic decays as indicated ensure that each atom will come to a steady state condition.

In the present analysis we use the following assumptions:

- (1) The decay rates of the transitions $a \rightarrow b$ (γ) and $a \rightarrow c$ (γ') are assumed to be the same (γ);
- (2) the probe field

*Corresponding author. Email address: ekuznetsova@rainbow.physics.tamu.edu

FIG. 1. Λ scheme under consideration.

is weak so that a first order analysis is valid; (3) the strong driving field is on resonance with the $a \rightarrow c$ transition.

The semiclassical Hamiltonian describing the atom-field interaction for the system under consideration can be written as

$$V = -\hbar\alpha e^{-i\nu t}|a\rangle\langle b| - \hbar\Omega e^{-i\nu_0 t}|a\rangle\langle c| + \text{H.c.}, \quad (1)$$

where $\Omega = \mu_{ac}E_d/2\hbar$ is the Rabi frequency of the drive field; the Rabi frequency of the probe field is defined by $\alpha = \mu_{ab}E_p/2\hbar$, μ_{ab} , and μ_{ac} are the matrix elements of the dipole moment between levels a and b and a and c , respectively; and ν and ν_0 are the frequencies of the probe and drive fields. The equations of motion for the density matrix elements are

$$\dot{\rho}_{ab} = -\Gamma_{ab}\rho_{ab} - i\alpha(\rho_{aa} - \rho_{bb}) + i\Omega\rho_{cb}, \quad (2a)$$

$$\dot{\rho}_{cb} = -\Gamma_{cb}\rho_{cb} - i\alpha\rho_{ca} + i\Omega\rho_{ab}, \quad (2b)$$

$$\dot{\rho}_{ac} = -\Gamma_{ac}\rho_{ac} - i\alpha\rho_{bc} - i\Omega(\rho_{aa} - \rho_{cc}), \quad (2c)$$

$$\dot{\rho}_{cc} = -w_{cb}\rho_{cc} + w_{ac}\rho_{aa} + w_{cb}\rho_{bb} - i\Omega(\rho_{ca} - \rho_{ac}), \quad (2d)$$

$$\dot{\rho}_{aa} = -(w_{ab} + w_{ac})\rho_{aa} - i\alpha(\rho_{ab} - \rho_{ba}) - i\Omega(\rho_{ac} - \rho_{ca}), \quad (2e)$$

$$\rho_{aa} + \rho_{bb} + \rho_{cc} = 1. \quad (2f)$$

Here the Rabi frequencies were assumed real, Γ_{ij} are defined as $\gamma_{ij} + i\Delta_{ij}$, w_{ij} are the population relaxation rates, $w_{cb} = w_{bc}$ so that before the action of the drive field the levels b and c are equally populated, and $\gamma_{ab} = \gamma_{ac} = \gamma$. The Δ_{ij} 's are given by $\Delta_{ab} = \omega_{ab} - \nu = \Delta + \Delta\omega_{ab}$, $\Delta_{ac} = \omega_{ac} - \nu_0 = \Delta_0 + \Delta\omega_{ac}$, $\Delta_{cb} = \omega_{cb} - \nu + \nu_0 = \Delta - \Delta_0 + \Delta\omega_{cb}$, and $\Delta\omega_{ac} = \Delta\omega_{ab} - \Delta\omega_{cb}$. Here ω_{ab} , ω_{ac} , and ω_{cb} are the frequencies of the corresponding transitions, $\Delta\omega_{ab}$ and $\Delta\omega_{cb}$ are the deviations of the atomic frequencies of the $a \rightarrow b$ and $c \rightarrow b$ transitions from the corresponding inhomogeneous line centers, and Δ and Δ_0 are the detunings of the probe and the drive fields from the line centers.

In the absence of the probe field the steady state solutions for the populations are obtained from Eqs. (2a)–(2f) as

$$\rho_{aa}^{(0)} = \frac{2w_{cb}\Omega^2}{2D}, \quad (3a)$$

$$\rho_{bb}^{(0)} = \frac{4\gamma X w_{cb} + 2w_{cb}\Omega^2 + 2\gamma\Omega^2}{2D}, \quad (3b)$$

$$\rho_{cc}^{(0)} = \frac{4\gamma X w_{cb} + 2w_{cb}\Omega^2}{2D}, \quad (3c)$$

where

$$X = \frac{\gamma^2 + \Delta_{ac}^2}{2\gamma},$$

$$D = 4\gamma X w_{cb} + \gamma\Omega^2 \left(1 + \frac{3w_{cb}}{w_{ac}}\right).$$

In terms of these populations ρ_{ab} can be found to first order in the probe field as

$$\rho_{ab} = \frac{-i\alpha}{\Gamma_{ab}\Gamma_{cb} + \Omega^2} \left[\Gamma_{cb}(\rho_{aa}^{(0)} - \rho_{bb}^{(0)}) + \frac{\Omega^2}{\Gamma_{ca}}(\rho_{cc}^{(0)} - \rho_{aa}^{(0)}) \right]. \quad (4)$$

Let us assume that the drive field is resonant, such that $\Delta_0 = 0$. Then ρ_{ab} can be written as

$$\rho_{ab} = \frac{-i\alpha}{Y} \frac{1}{2D} \left[-(\gamma_{cb} + i\Delta_{cb})(4X\gamma w_{cb} + 2\Omega^2\gamma) + \frac{\Omega^2}{\gamma - i\Delta\omega_{ac}} 4\gamma X w_{cb} \right], \quad (5)$$

where

$$Y = (\gamma + i\Delta + i\Delta\omega_{ab})(\gamma_{cb} + i\Delta_{cb}) + \Omega^2.$$

In an inhomogeneously broadened solid system, the susceptibility should be averaged over the entire range of the frequencies of the corresponding transition, which is determined by the inhomogeneity of the crystalline fields in solids. Similarly, in EIT experiments in gases the inhomogeneous Doppler broadening at the optical transitions should be taken into account [16]. Inhomogeneous broadening at the low-frequency (hyperfine or Zeeman) transition, caused by the residual Doppler effect $(k_2 - k_1)v$, can be neglected as compared to the homogeneous width of the transition determined by the time of flight of an atom through a laser beam, because $\omega_{cb} \ll \omega_{ab}, \omega_{ac}$. However, in EIT experiments in solids (as well as in gases with large ω_{cb} [17]) inhomogeneous broadening at both one-photon and two-photon transitions plays an important role. Averaging of the susceptibility over inhomogeneous profiles is described in the Appendix.

III. EIT LINEWIDTH

In order to estimate the linewidth of the EIT resonance we evaluate the imaginary part of the susceptibility, which is the sum of three terms $\chi'' = \chi''_{11} + \chi''_{12} + \chi''_{21}$, calculated in the Appendix.

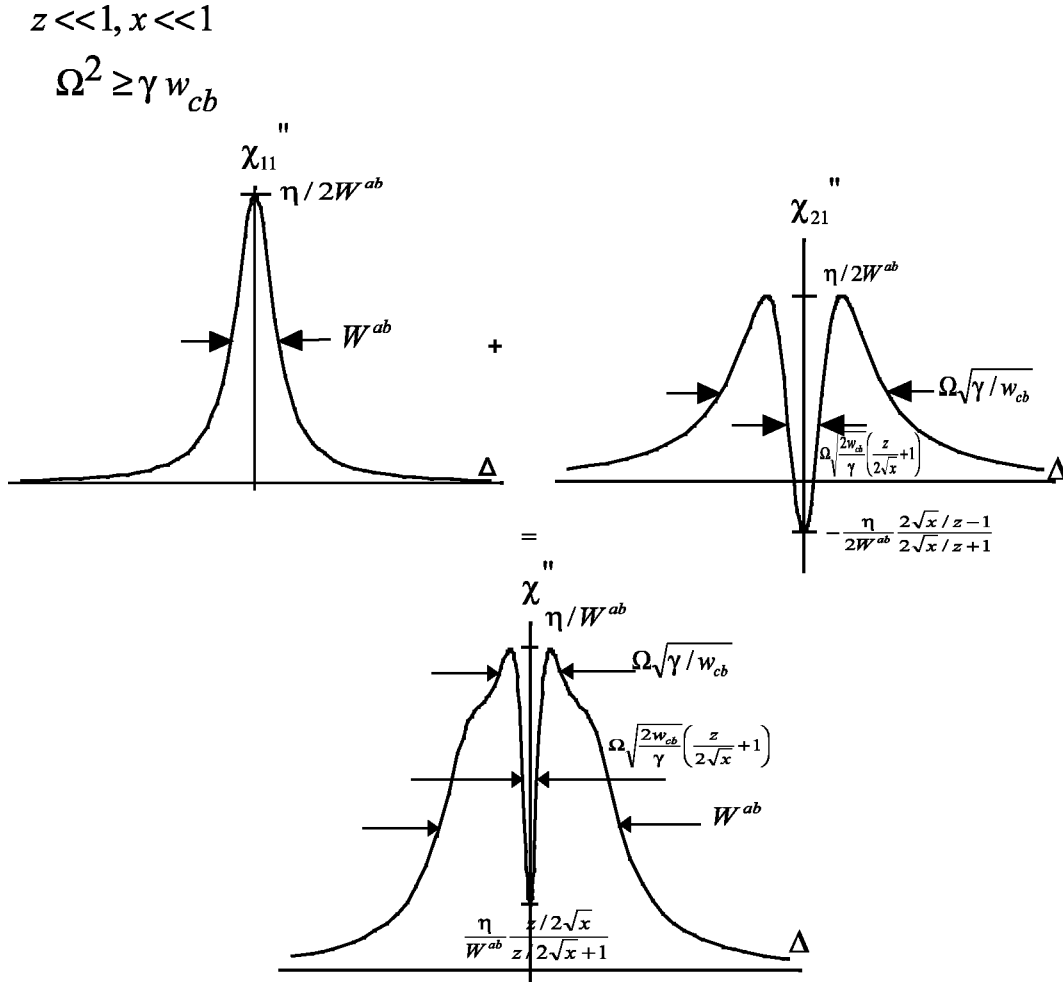


FIG. 2. A numerical calculation of susceptibility components under conditions $z \ll 1$, $x \ll 1$, $\Omega^2 \geq \gamma w_{cb}$. An antihole forms in χ''_{21} and is clearly seen in the resulting χ'' profile.

The susceptibility strongly depends on two parameters:

$$x = \frac{\Omega^2 \gamma}{2w_{cb}(W^{ab})^2},$$

$$z = \frac{\gamma W^{cb}}{w_{cb} W^{ab}}, \quad (6)$$

where $2W^{ab(cb)}$ is the width of the inhomogeneously broadened optical (low-frequency) transition. The parameter x can be presented in the form $x = \Omega^2/\Omega_{inh}^2$, where $\Omega_{inh}^2 = 2w_{cb}(W^{ab})^2/\gamma$ gives the characteristic value of the drive field intensity ($I_{inh} \sim \Omega_{inh}^2$) providing optical pumping for all atoms within an inhomogeneously broadened optical line. Hence the parameter x defines the degree of optical pumping of atoms into the ground state.

The parameter z is defined by the ratio of the relative broadenings at the low-frequency and optical transitions. In a gaseous medium in the Λ scheme with copropagating fields, where inhomogeneous broadening at the low-frequency transition [defined by the residual Doppler effect $(k_2 - k_1)v$] is negligible (and hence W^{cb} should be replaced by w_{cb}), this

parameter takes the form $z = \gamma/W^{ab}$, i.e., it does not exceed 1. In a Bose-Einstein condensate $z = 1$. In a solid medium it may be either less than or greater than 1, depending on the magnitude of the inhomogeneous broadening at the low-frequency transition characterizing the dephasing between spins of different ions.

Usually the inhomogeneous broadening at a spin transition is orders of magnitude smaller than at an optical transition. Hence the term χ''_{12} , which is W^{cb}/W^{ab} times smaller than χ''_{11} , can be neglected.

Typical shapes of χ''_{11} and χ''_{21} for different regimes of EIT are shown in Figs. 2–6.

In order to estimate the linewidth of the EIT resonance we first find that the maximum of $\chi'' = \chi''_{11} + \chi''_{21}$ is $\chi''_{max} \approx \eta/W^{ab}$ at $\Delta \approx \pm \Omega$. As the next step we calculate the minimum absorption at zero detuning, of the probe field which is given by the expression

$$\chi''(\Delta=0) = \frac{\eta}{W^{ab}} \frac{x + z/2 + z\sqrt{x}/2}{(1 + \sqrt{x})(x + z/2)(1 + 2\sqrt{x}/z)}. \quad (7)$$

Let us define Γ_{EIT} as $\chi''(\Delta = \Gamma_{EIT}) = [\chi''_{max} + \chi''(\Delta = 0)]/2$. Then the width of the EIT resonance is obtained as

$$z \ll 1, \quad x \gg 1$$

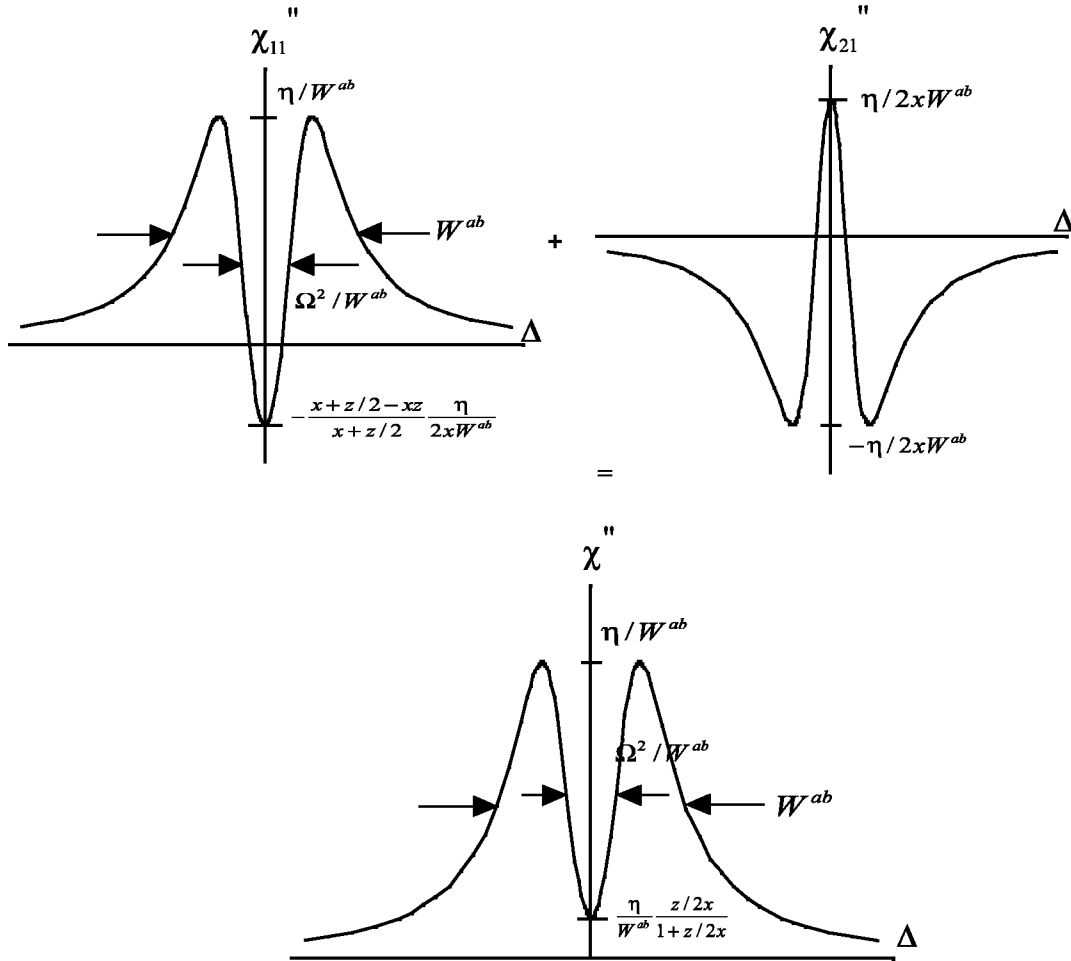


FIG. 3. Susceptibility components under conditions $z \ll 1, x \gg 1$. EIT resonance is power broadened.

$$\Gamma_{EIT}^2 = \frac{2\sqrt{x}}{z} (W^{cb})^2 \frac{[1+x\sqrt{x}+2x(1+x)/z][1+\sqrt{x}/z+x/z]}{x+\sqrt{x}+1+2x(1+\sqrt{x})/z} \times \left[1 + \left\{ 1 + \frac{z^2}{4x} \frac{(1+2x/z)^2(1+2\sqrt{x}/z)^2[x+\sqrt{x}+1+2x(1+\sqrt{x})/z]^2}{[1+x\sqrt{x}+2x(1+x)/z]^2(1+\sqrt{x}/z+x/z)^2} \right\}^{1/2} \right]. \quad (8a)$$

Let us define also the transmission coefficient T as

$$T = \exp \left[- \frac{2\pi kL\eta}{W^{ab}} \times \frac{1+\sqrt{x}+2x/z}{(1+\sqrt{x})(1+2x/z)(1+2\sqrt{x}/z)} \right], \quad (8b)$$

where $k = \nu c$ is the wave number of the probe field, L is the length of the medium, and $\eta = N\mu_{ab}^2/2\hbar$.

The threshold intensity of the driving field providing EIT and the dependence of the EIT linewidth broadening and the

transmission coefficient on the intensity are essentially determined by the parameter z . Let us analyze two extreme limits: $z \ll 1$ and $z \gg 1$.

A. $z \ll 1$

This limit might be realized in solids with a relatively small inhomogeneous width W^{cb} of the low-frequency transition.

For low intensities of the drive laser ($x \ll 1$) the second term χ''_{21} gives an antihole (see Fig. 2), formed due to absorption by the atoms resonantly pumped from the state c to the ground state b . The width of the antihole is defined by the

$$z \gg 1, x \ll 1$$

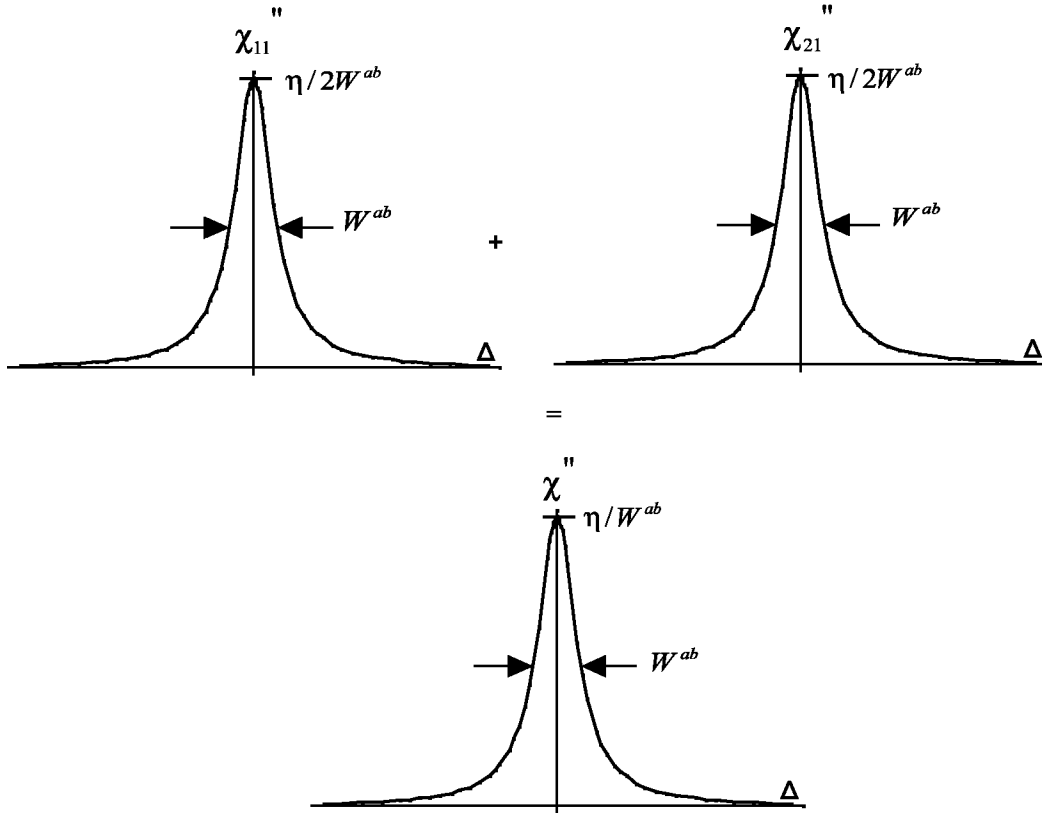


FIG. 4. Susceptibility components in the case $z \gg 1$, $x \ll 1$. There is no EIT in this regime.

magnitude of the maximal detuning for which atoms are optically pumped for a given intensity: $\Delta_{ant} = \Omega \sqrt{\gamma/w_{cb}}$. This antihole is imposed on a broad background with the width W^{ab} representing the absorption of off-resonant atoms, which is described by the term χ''_{11} .

The line center absorption in this limit is $\chi''(\Delta=0) \approx \eta/[W^{ab}(1+2\sqrt{x}/z)]$, so EIT becomes observable as $\sqrt{x}/z \sim 1$ or $\Omega^2 \sim \gamma(W^{cb})^2/w_{cb}$. As long as this condition is satisfied, $\chi''(\Delta=0)$ is vanishingly small as $\eta z/2W^{ab}\sqrt{x}$ when $x \ll 1$ and as $\eta z/2W^{ab}x$ when $x \gg 1$.

The linewidth for low drive laser intensity, when only some of the atoms (with detunings within the antihole width) are optically pumped into the state b , i.e., $x \ll 1$, is

$$\Gamma_{EIT}^2 = \frac{2\sqrt{x}}{z} (W^{cb})^2 (1 + \sqrt{x}/z) \times \left[1 + \left\{ 1 + \frac{(1 + z/2\sqrt{x})^2}{(1 + \sqrt{x}/z)^2} \right\}^{1/2} \right].$$

As EIT sets in with $\sqrt{x}/z \sim 1$, the linewidth is $\Gamma_{EIT} \sim W^{cb}$. Note that, generally speaking, the threshold intensity [$\Omega^2 \sim \gamma(W^{cb})^2/w_{cb}$] is larger than that in a homogeneously broadened medium ($\Omega^2 \sim \gamma\gamma_{cb}$) by a factor $(W^{cb})^2/\gamma_{cb}w_{cb} > 1$. For higher intensities, when $\sqrt{x}/z \gg 1$ but still $x \ll 1$, we easily obtain

$$\Gamma_{EIT} \Rightarrow \Omega \sqrt{\frac{2w_{cb}}{\gamma}}. \quad (9a)$$

According to Eq. (9a) the linewidth of EIT is linearly proportional to Ω , the Rabi frequency of the driving field (i.e., the square root of the intensity) and is independent of the inhomogeneous width W^{ab} . For very high intensities of the drive laser ($x \gg 1$) when all atoms are optically pumped into the state b the general formula (8a) takes the form of the traditional power broadening law:

$$\Gamma_{EIT} \Rightarrow \frac{\Omega^2}{W^{ab}}. \quad (9b)$$

In Fig. 7 the EIT linewidth and transmission coefficient dependence on the characteristic combination of parameters $2\sqrt{x}/z = \Omega \sqrt{2w_{cb}/\gamma(W^{cb})^2}$ in the case $z \ll 1$ is highlighted. The logarithmic plot shows that at low intensity of the drive laser ($2\sqrt{x}/z < 1$) the width is constant, but at higher ($2\sqrt{x}/z > 1$) intensity it changes along a line with slope 1, and at even higher intensity ($2\sqrt{x}/z \sim 10^2$) the slope changes to 2.

It is worth noting that, with the introduction of an effective width δ_{eff} defined as the magnitude of the maximum detuning for which atoms are optically pumped into the ground state b , the EIT linewidth can always be presented in

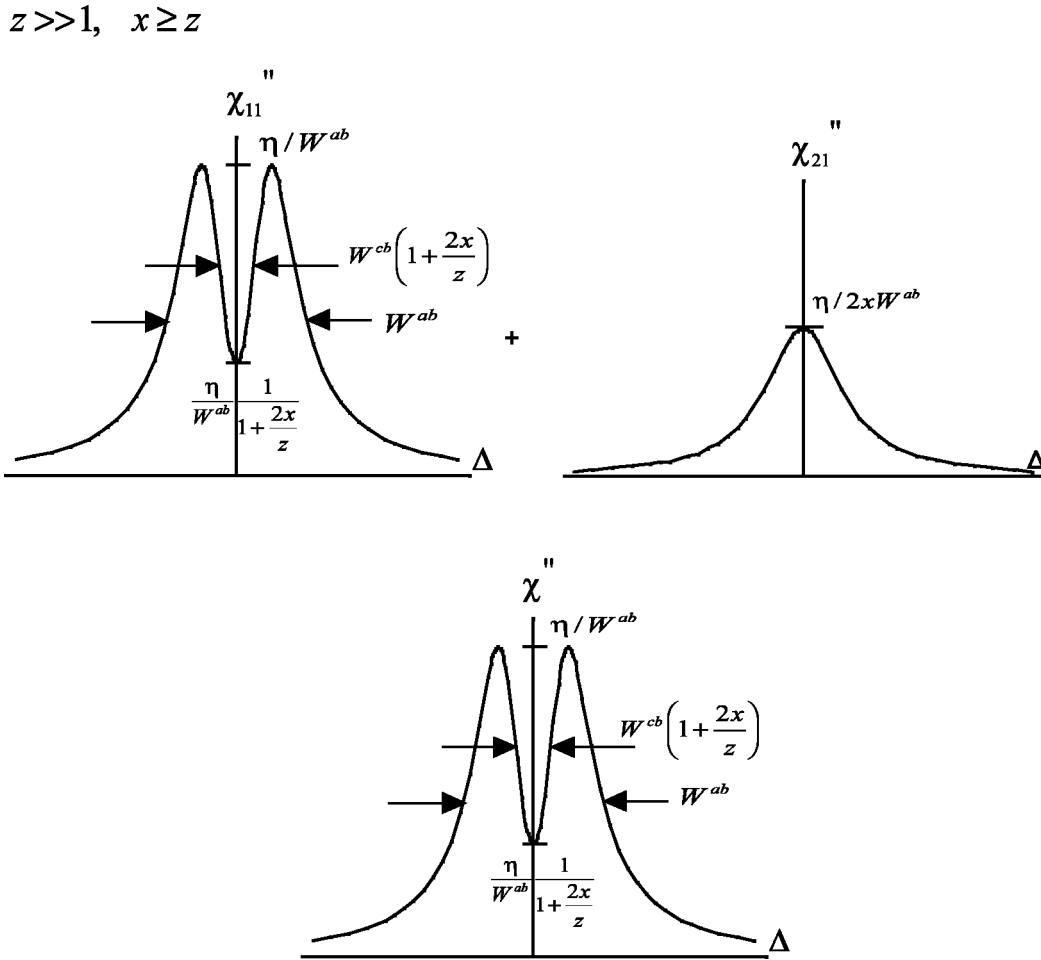


FIG. 5. Susceptibility in the case $z \gg 1, x \geq z$. EIT sets in when the drive laser intensity exceeds a threshold value ($\Omega^2 > W^{ab}W^{cb}$); EIT resonance is power broadened.

the form $\Gamma_{EIT} = \Omega^2 / \delta_{eff}$, which is similar to the EIT linewidth in a homogeneously broadened medium, where $\Gamma_{EIT} = \Omega^2 / \gamma$.

The physical reason for a linear dependence of the EIT linewidth on Ω in the case $x \ll 1$ is that δ_{eff} (which is defined in this range of intensities by the width of the antihole) is proportional to Ω , i.e., more and more far-detuned atoms become optically pumped into the ground state. On the other hand, at very high intensity ($x \gg 1$), when all atoms are optically pumped and hence δ_{eff} does not increase any more after reaching its maximum value at $x=1, W^{ab}$, the EIT linewidth broadens proportionally to the intensity.

A similar linear dependence on Ω [see Eq. (9a)] of the width of some sub-Doppler resonances was obtained in earlier work by Feld and Javan in three-level laser gain systems [18]. In the situation under study in [18] the relaxation rates at the one-photon and two-photon transitions were of the same order, so that the resonance width was fully determined by the Rabi frequency in the whole range of intensities. A linear dependence of the EIT linewidth on the drive field Rabi frequency was found in [16], where inhomogeneous broadening at the two-photon transition was ignored, and also in [19] [although in a different regime corresponding to trapping of all atoms ($\gamma_{bc} = 0$) and with a relatively strong

signal field contributing to the line broadening].

We are not aware of any experimental reports of linear dependence of the EIT linewidth on the Rabi frequency except for two recent sets of experiments in a Rb cell by Zibrov [20] corresponding, respectively, to (i) the frequency-selective CPT regime described in this work and (ii) the signal-broadened EIT regime of [19].

The quadratic dependence formula (9b) was obtained earlier in [21] under the assumption that all atoms were optically trapped. As is clear from the above analysis, this assumption holds when $x \gg 1$.

Apparently, the smaller ratio γ_{bc} / γ leads to a smaller EIT width at $x \ll 1$ and to smaller value of Ω for which the linear dependence ($\Gamma_{EIT} \sim \Omega$) changes to a quadratic dependence ($\Gamma_{EIT} \sim \Omega^2$).

Note that at an arbitrary fixed value of intensity and given homogeneous broadening the EIT linewidth in an inhomogeneously broadened medium ($\Gamma_{EIT} = \Omega^2 / \delta_{eff}$) is essentially narrower than in a homogeneously broadened medium ($\Gamma_{EIT} = \Omega^2 / \gamma$). The physical reason for this EIT line-narrowing effect is that power broadening of the line is weaker for off-resonant atoms. This line-narrowing effect is similar to that discussed earlier by Feld and Javan [18]. At the same time the EIT linewidth can never be reduced beyond its ultimate limit defined by W^{cb} .

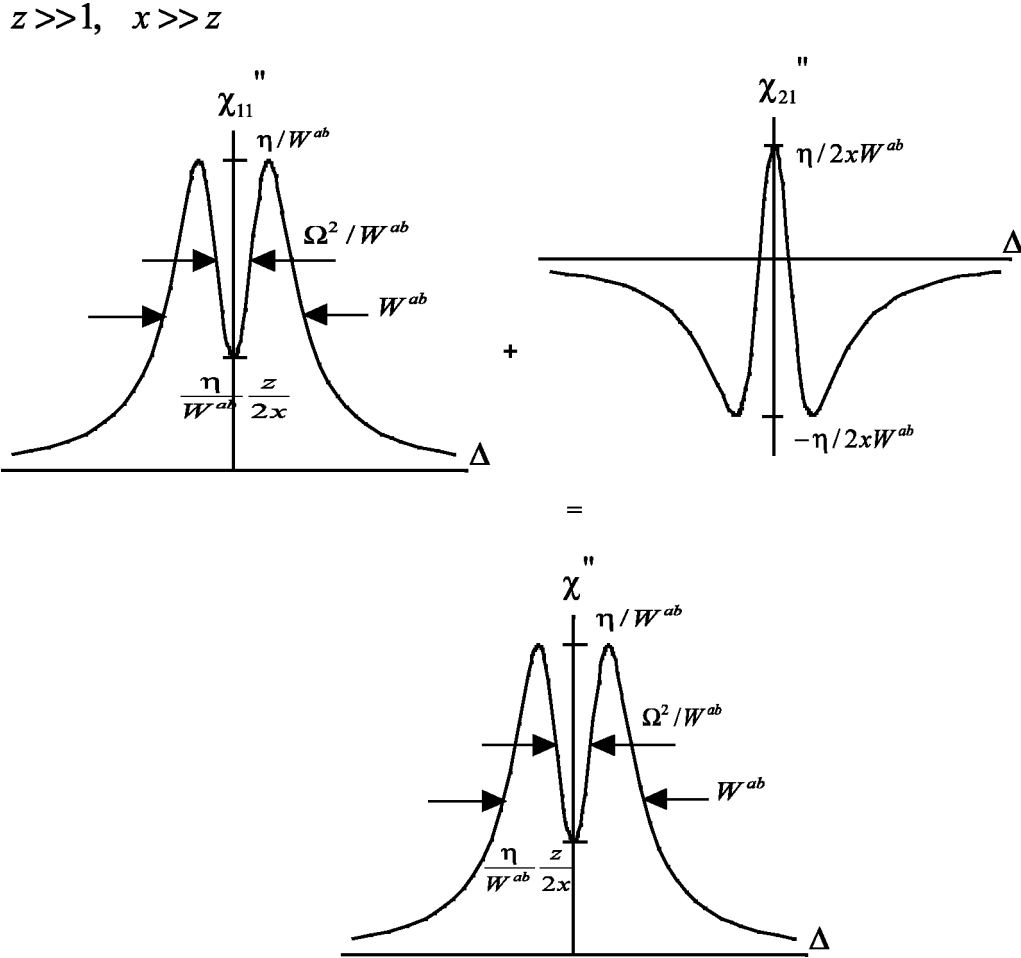


FIG. 6. A numerical calculation of susceptibility under conditions $z \gg 1, x \gg z$. EIT amplitude is 100%; the resonance is power broadened.

B. $z \gg 1$

Here no EIT is observed until $x \sim z$, when $\chi''(\Delta=0) \approx \eta/[W^{ab}(1+2x/z)]$; for $x \gg z$ absorption at the line center is small as $\eta z/2W^{ab}x$.

The corresponding linewidth for low intensity is

$$\Gamma_{EIT}^2 = \frac{2x}{z} (W^{cb})^2 (1+x/z) \times \left[1 + \left\{ 1 + \frac{(1+z/2x)^2}{(1+x/z)^2} \right\}^{1/2} \right],$$

so again EIT starts with $\Gamma_{EIT} \sim W^{cb}$, but in this case with much higher intensity $\Omega^2 \sim W^{ab}W^{cb}$ ($x \sim z$). For higher intensities ($x \gg z$)

$$\Gamma_{EIT} \Rightarrow \frac{\Omega^2}{W^{ab}}.$$

For media with a large inhomogeneous width of the $c \rightarrow b$ transition, characterized by the condition $z \gg 1$, we see that a considerably higher (by the factor $W^{ab}W^{cb}/\gamma\gamma_{cb}$) intensity is required for EIT to be observed than in a homogeneously

broadened medium, and there is no linear dependence on the Rabi frequency of the drive field as we found in the limit $z \ll 1$. From the very beginning, when the intensity of the drive laser exceeds the threshold intensity ($\Omega^2 \sim W^{ab}W^{cb}$) the linewidth is power broadened.

IV. GROUP VELOCITY IN AN INHOMOGENEOUSLY BROADENED EIT MEDIUM

The dispersive properties of an electromagnetically induced transparent medium are as interesting as its absorption characteristics. It has been demonstrated both theoretically [22] and experimentally [14,23–25] that EIT is accompanied by steep frequency dispersion (large derivative $dn/d\nu$) near the line center, which leads to a time delay of the probe pulse and reduction in its group velocity. As is well known the group velocity of light in a medium is given by

$$V_g = \frac{c}{n + \nu dn/d\nu},$$

where $n \approx n_0 + 2\pi\chi'$.

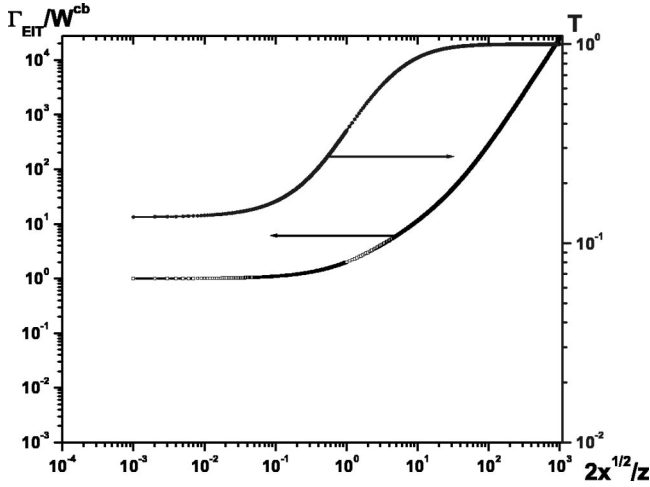


FIG. 7. Logarithmic plots illustrating EIT linewidth and transmission dependence on the characteristic parameter $2\sqrt{x}/z$ in the case $z \ll 1$.

In the experimental conditions of Refs. [8,14,23–26] the refractive index $n_0 \sim 1-2$ and in the EIT regime we can neglect n_0 in comparison with $\nu dn/d\nu$, so that $V_g = c/(2\pi\nu d\chi'/d\nu)$.

The time delay for a pulse in a sample of length L is then

$$T_D = L(1/V_g - 1/c) = \frac{2\pi\nu L}{c} \frac{\partial\chi'}{\partial\nu}.$$

For the inhomogeneously broadened system considered in Sec. II the steepness of the dispersion function is given by the expression

$$\left. \frac{\partial\chi'}{\partial\nu} \right|_{\nu=\omega_{ab}} = \frac{\eta}{W^{ab}W^{cb}} \frac{2\sqrt{x}/z}{1+\sqrt{x}} \times \frac{1+\sqrt{x}+x+4x(1+\sqrt{x})/z+4x^2/z^2}{(1+2\sqrt{x}/z)^2(1+2x/z)^2}.$$

Let us again consider limits $z \ll 1$ and $z \gg 1$.

A. $z \ll 1$

For low drive field intensities ($x \ll 1$) EIT becomes observable when $\sqrt{x} \sim z$, and

$$\left. \frac{\partial\chi'}{\partial\nu} \right|_{\nu=\omega_{ab}} \approx \frac{\eta}{W^{ab}} \frac{2\sqrt{x}/z}{W^{cb}} = \frac{\eta}{W^{ab}} \frac{2\sqrt{x}}{z} \frac{1}{\Gamma_{EIT}}.$$

When $x \ll 1$ and $\sqrt{x} \gg z$

$$\left. \frac{\partial\chi'}{\partial\nu} \right|_{\nu=\omega_{ab}} \approx \frac{\eta}{W^{ab}} \frac{1}{\Omega\sqrt{2W^{cb}/\gamma}} = \frac{\eta}{W^{ab}} \frac{1}{\Gamma_{EIT}}.$$

For high drive laser intensities corresponding to $x \gg 1$ the steepness is

$$\left. \frac{\partial\chi'}{\partial\nu} \right|_{\nu=\omega_{ab}} \approx \frac{\eta}{\Omega^2} = \frac{\eta}{W^{ab}} \frac{W^{ab}}{\Omega^2} = \frac{\eta}{W^{ab}} \frac{1}{\Gamma_{EIT}}.$$

B. $z \gg 1$

In this limit EIT becomes observable when $x \sim z$. At this time

$$\left. \frac{\partial\chi'}{\partial\nu} \right|_{\nu=\omega_{ab}} \approx \frac{\eta}{W^{ab}} \frac{2x/z}{(1+2x/z)^2} \frac{1}{W^{cb}} = \frac{\eta}{W^{ab}} \frac{2x/z}{(1+2x/z)^2} \frac{1}{\Gamma_{EIT}}.$$

For $x \gg z$,

$$\left. \frac{\partial\chi'}{\partial\nu} \right|_{\nu=\omega_{ab}} \approx \frac{\eta}{\Omega^2} = \frac{\eta}{W^{ab}} \frac{W^{ab}}{\Omega^2} = \frac{\eta}{W^{ab}} \frac{1}{\Gamma_{EIT}}.$$

As we can see, in general case under EIT conditions the group velocity and accordingly the time delay of the pulse are defined as

$$V_g/c = \frac{1}{\pi\omega} \frac{\hbar\Gamma_{EIT}W^{ab}}{N\mu_{ab}^2}, \quad (10)$$

$$T_D = \frac{\pi\omega L}{c} \frac{N\mu_{ab}^2}{\hbar W^{ab}\Gamma_{EIT}}.$$

Note that it is this last parameter T_D which also defines the efficiency of the nonlinear transformations. So when the drive field intensity exceeds a threshold value and EIT sets in, it is followed by steep dispersion, which is inversely proportional to the EIT linewidth Γ_{EIT} . In its turn, the group velocity of the probe pulse is linearly proportional to the EIT width. So the smaller Γ_{EIT} , the slower the group velocity of light, which is fundamentally limited by the coherence lifetime γ_{cb} in a Doppler-broadened gaseous medium or by the inhomogeneous broadening of the low-frequency transition W^{cb} in a solid medium.

Let us note also that the group velocity is proportional to the parameter η , i.e., to the product of $N\mu_{ab}^2$, and inversely proportional to W^{ab} . So it is clear that the use of a repump field, as in the experiment [8], does not allow one to reduce the group velocity. It does allow one to reduce the inhomogeneous linewidth by the factor $W^{ab}/\Delta\nu_{jit}$. However, at the same time the effective density of the atoms is reduced by the same factor.

V. COMPARISON OF THE THEORY WITH THE EXPERIMENTS ON EIT AND SGV

In this part of the paper we want to compare recent experiments on EIT and SGV with the results of the above theory. In Refs. [8,11] EIT was observed in a rare-earth doped crystal (Pr^{3+} -doped Y_2SiO_5 or $\text{Pr}:\text{YSO}$), and in N - V color centers in diamond respectively. All relevant experi-

TABLE I. The experimental parameters.

	$2W^{ab}$ (GHz)	$2W^{cb}$ (kHz)	w_{ab}^{-1} (μ s)	γ_{ab}^{-1} (μ s)	$\Delta\nu_{jit}$ (MHz)
Pr:YSO	4	60	164	111	1
<i>N-V</i> diamond	750	5.5×10^3	1.3×10^{-2}	3.3×10^{-3}	100
	w_{cb}^{-1} (s)	γ_{cb}^{-1} (μ s)	λ (nm)	f	I (W/cm ²)
Pr:YSO	100	500	605.7	3×10^{-7}	90
<i>N-V</i> diamond	5×10^{-3}	40	637	0.1	280

mental parameters are listed in Table I. Here w_{ab}, w_{cb} are the population relaxation and γ_{ab}, γ_{cb} are the coherence relaxation times for $a \rightarrow b$ and $c \rightarrow b$ transitions; $\Delta\nu_{jit}$ is the laser jitter; λ is the linewidth of the $a \rightarrow b$ transition; f is the optical transition oscillator strength; and I is the intensity of the drive laser.

Given the oscillator strength, the dipole moment of the optical transition can be estimated as

$$\mu_{ab}^2 = f \frac{e^2}{\hbar c} \frac{\hbar^2 \lambda}{4\pi m_e}, \quad (11)$$

and, based on the intensity of the drive field, its Rabi frequency is

$$\Omega = \frac{\sqrt{2\pi}\mu_{ab}}{\hbar\sqrt{cn_0}}\sqrt{I}.$$

We estimated the Rabi frequency used in Ref. [8] to be 500 kHz for $I=90$ W/cm²; in Ref. [11] the Rabi frequency 160 MHz is cited. The density of Pr ions in [8] was $N=4.7 \times 10^{18}$ cm⁻³ and the absorption coefficient was $\alpha=10$ cm⁻¹; for the *N-V* color centers in [11] the density of centers was $N=3 \times 10^{18}$ cm⁻³ and the peak optical density was ~ 0.3 .

In Ref. [8] the system was rather six level than three level, and an additional repump field was used, which made only a small fraction of Pr ions, confined within the laser linewidth, interact with the laser fields. For these ions a six-level system was reduced to a three-level Λ scheme with the laser jitter serving as an effective inhomogeneous broadening at the optical transitions. Accordingly, the effective density of Pr ions

TABLE II. The experimental and calculated EIT linewidth, transmission and group velocities for EIT in solid media experiments.

	Γ_{EIT}^{expt} (kHz)	Γ_{EIT}^{calc} (kHz)	T^{expt} (%)	T^{calc} (%)	z	x	V_g^{expt} (m/s)	V_g^{calc} (m/s)
Pr ³⁺ :YSO	30	46	36	26	3×10^4	10^5	45	8000
<i>N-V</i> diamond	8500	7800	70	11	5	0.1		470

TABLE III. The experimental parameters of EIT in gaseous media experiments.

	W^{ab} (MHz)	W^{cb} (kHz)	γ_{ab} (MHz)	w_{ab} (MHz)	w_{cb} (Hz)
Ref. [14]	270	10^3	150	3	10^3
Ref. [23]	10	20	10	10	1.6×10^4
	γ_{cb} (Hz)	λ (nm)	I (mW/cm ²)	N (cm ⁻³)	f
Ref. [14]	10^3	795	10	2×10^{12}	0.33
Ref. [23]	1.6×10^4	589	12	8×10^{13}	1

with laser jitter was $4.7 \times 10^{18} \times 10^6 / (4 \times 10^9) = 1.17 \times 10^{15}$ cm⁻³ or even less depending on the intensity of the repump laser.

The experimental and calculated values of the EIT linewidth and transmission T and estimates for parameters z and x are given in Table II. As we can see, the theoretically calculated values of the EIT linewidth are close to the experimental values. There is also good matching for the experimental and theoretical values of the transmission coefficient in Pr:YSO. The discrepancy in the observed and calculated transmissions for Ref. [11] (about seven times) is probably due to the use of a repump laser, necessary to prevent reorientation of the *N-V* centers in the diamond lattice.

Using the relation between the dipole moment and oscillator strength (11) the ratio of the group velocity to the speed of light, according to Eq. (10), is

$$V_g/c = \frac{2m_e}{\pi\hbar c} \frac{1}{f} \frac{\hbar c}{e^2} \frac{1}{N/(\Gamma_{EIT}W^{ab})}. \quad (12)$$

A group velocity of the order of 1–10 m/s has been achieved in recent experiments in gases. The parameters and results for the group velocity in gases are summarized in Tables III, and IV. As it is clear from Table IV, they are in good correspondence with the theoretical calculations on the basis of Eq. (12). Note that in the experiment [23] the Rabi frequency of the drive laser was an order of magnitude greater than the coherent threshold Rabi frequency at which EIT starts, so the resonance was power broadened, which means that $\Gamma_{EIT} = \Omega^2/\gamma_{ab}$. If it were not power broadened, the EIT width would be just the coherence relaxation rate of the low-frequency transition γ_{cb} , which would lead to $V_g/c \approx 1.3 \times 10^{-10}$ ($V_g \approx 6$ cm/s).

Let us compare now the group velocity, observed in a recent experiment in Pr³⁺:YSO [26], with the prediction of the above theory. The results are given in Table II and in Fig. 8. In Table II we list the experimental value of the group

TABLE IV. The experimental and calculated group velocities for EIT experiments in gaseous media.

	Ref. [14]	Ref. [23]	Ref. [25]
V_g^{expt} (m/s)	90	17	8
V_g^{calc} (m/s)	350	21	5

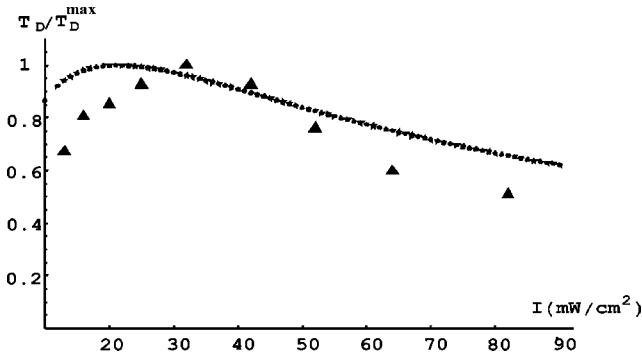


FIG. 8. Experimentally observed (triangles) and calculated (stars) time delay for $\text{Pr}^{3+}:\text{YSO}$ [26].

velocity of 45 m/s and the corresponding calculated value of 8000 m/s. Taking into account the very good coincidence between theoretical predictions and experimental results for the EIT linewidth and transmission coefficient in $\text{Pr}:\text{YSO}$ (Table II), the origin of the large difference in V_g (about 180 times) remains unclear. A possible explanation of this discrepancy may be the square shape of the probe pulses used in [26]. A pulse of this shape is considerably modified during propagation in a resonant medium, which may cause an uncertainty in the actual delay time and group velocity. A more detailed comparison with this experiment is shown in Fig. 8, where calculated and experimentally observed group velocities (normalized to their maximum values) are given for a range of driving field intensities. We can see that the experimentally observed and theoretically calculated curves look very similar to each other. Also, in Table II we give the theoretical predictions for the possible group velocity in another solid medium, namely, N - V color centers in diamond, where EIT was observed recently [11], but the group velocity has not been measured yet.

VI. SOLIDS VS GASES: POTENTIAL ADVANTAGES OF SOLIDS

As is clear from the above discussion, the minimum value of the EIT linewidth is defined by W^{cb} and it is achieved when the intensity of the drive laser is about the threshold value needed to observe EIT. In order to minimize inhomogeneous broadening at the spin transition it is preferable to use hyperfine rather than Zeeman splitting, choosing a lattice with zero nuclear spin. In some rare-earth doped crystals (for example, $\text{Eu}^{2+}:\text{CaF}_2$, $\text{Pr}^{3+}:\text{Y}_2\text{SiO}_5$, N - V color centers in diamond) W^{cb} can be of the order of 1–10 kHz, i.e., of the same order of magnitude as in some EIT experiments in hot gases [14] and Bose-Einstein Condensates (BEC's) [23], where it is typically defined by the time of flight of atoms through a laser beam. However, W^{cb} in solid materials cannot overcome the record value of 1 Hz achieved in experiments with a paraphine coated Rb cell [25].

The EIT threshold intensity in an inhomogeneously broadened medium in general is higher than that in a homogeneously broadened medium ($\Omega^2 > \gamma\gamma_{cb}$) by the factor $(W^{cb})^2/\gamma_{cb}W_{cb}$ if $z < 1$ or by the factor $W^{ab}W^{cb}/\gamma\gamma_{cb}$ if $z > 1$. Note that for solids with $z < 1$ it does not depend on

W^{ab} , while for solids with $z > 1$ it is proportional to the inhomogeneous broadening of an optical transition. The typical value of the threshold intensity for gaseous media with the parameters listed in Table III is of the order of mW/cm^2 , while in experimental work with solids with the parameters listed in Table I it is of the order of 10^2 – $10^5 \text{ W}/\text{cm}^2$. The way to reduce the requirement for the threshold intensity is to use materials with the smallest possible inhomogeneous broadening of the spin transition. In the case $z > 1$ it is reasonable also to use electric-dipole allowed optical transitions in combination with the smallest possible inhomogeneous broadening of the optical transition. There is a wide class of rare-earth doped dielectrics possessing a zero-phonon line at low temperature (up to 10 K) at the electric-dipole allowed f - d transitions lying in the band gap of a host matrix. Some examples include $\text{Yb}^{3+}:\text{LiYF}_4$, $\text{Yb}^{2+}:\text{MgF}_2$, $\text{Pr}^{3+}:\text{Cs}_2\text{NaYCl}_6$, $\text{Ce}^{3+}:\text{Cs}_2\text{NaYCl}_6$, $\text{Ce}^{3+}:\text{LuPO}_4$, $\text{Ce}^{3+}:\text{YPO}_4$, $\text{Ce}^{3+}:\text{YAG}$, $\text{Ce}^{3+}:\text{CaSO}_4$, $\text{Tb}^{3+}:\text{LiYF}_4$, $\text{Eu}^{2+}:\text{CaS}$, $\text{Eu}^{2+}:\text{MgS}$, $\text{Eu}^{2+}:\text{MgF}_2$, $\text{Eu}^{2+}:\text{CaF}_2$, $\text{Np}^{4+}:\text{ZrSrO}_4$, $\text{Pa}^{4+}:\text{Cs}_2\text{ZrCl}_6$. Although the inhomogeneous width of a dipole allowed optical transition is usually greater than that of a dipole forbidden transition, there is no linear relation between the dipole moment and the inhomogeneous width, so the latter can be reduced by controlling the purity of the crystal sample. There are some rare earths, namely, Pr^{3+} [27], Ce^{3+} [28,29], Eu^{2+} [30,31], and Tb^{3+} [32], whose dipole allowed f - d transitions in different hosts have relatively small inhomogeneous optical line broadening, ranging from 40 to 300 GHz. Note that inhomogeneous line broadening can be effectively reduced up to the magnitude of the laser beam jitter (which can be as small as 1 kHz [33]) using an optical repump scheme as was done in [8]. This effectively reduces the requirement for the EIT threshold intensity. The price to be paid for this is a corresponding reduction in the effective atomic density of the dopants participating in the EIT.

Let us now compare the dispersive properties of EIT in gases and solids in order to estimate the potential of solid materials for the slowing of light and realization of nonlinear interactions.

On the basis of Eq. (12) the general recipe for achieving a slow group velocity is using the highest possible dopant density, electric-dipole allowed transitions, and the smallest possible inhomogeneous line broadening at both the spin and optical transitions.

One of the major advantages of solids as compared to gases is the high concentration. The concentration of dopants in solids can be much greater (about 10^{18} – 10^{22} cm^{-3}) than the atomic density in gases (about 10^{10} – 10^{13} cm^{-3}) for which atomic collisions do not broaden the optical and spin transitions. This is crucial for the slowing of light and for the efficiency of nonlinear processes.

Taking a combination of favorable parameters such as the density of impurity atoms of $N \sim 10^{22} \text{ cm}^{-3}$, the inhomogeneous width of the spin transition $W^{cb} \sim 10 \text{ kHz}$, and the inhomogeneous width of the dipole allowed ($f \sim 0.1$) optical transition $W^{ab} \sim 50 \text{ GHz}$, and assuming that the EIT resonance is not power broadened, one can obtain

$$V_g/c \approx 10^{-13} \quad (V_g \approx 30 \text{ } \mu\text{m/s}).$$

Unfortunately in real materials it is difficult to realize such a favorable combination of parameters.

Let us consider Ce^{3+} doped crystals like YAG, LuPO_4 , YPO_4 , YLiF_4 , and $\text{Cs}_2\text{NaYCl}_6$. The relatively high oscillator strength $f \sim 10^{-4}$ in these materials is nicely combined with relatively small inhomogeneous broadening of the optical transition: $W^{ab} \sim 100 \text{ GHz}$ [34,35]. Unfortunately, there is no hyperfine structure (the spin of Ce nuclei is zero) and inhomogeneous broadening at the Zeeman transition is typically rather large: $W^{cb} \sim 1\text{--}10 \text{ MHz}$ [36]. At the density of dopants $N = 10^{20} \text{ cm}^{-3}$, it would give us $V_g \approx 200 \text{ m/s}$. The required intensity to observe EIT in such crystal would be rather high, $I_{thres} \approx 5 \text{ kW/cm}^2$.

Another example is Eu^{2+} doped crystals like $\text{Eu}^{2+}:\text{CaF}_2$, $\text{Eu}^{2+}:\text{SrF}_2$, $\text{Eu}^{2+}:\text{MgF}_2$, and $\text{Eu}^{2+}:\text{MgS}$. In these materials inhomogeneous broadening of the spin transition is rather small $W^{cb} \sim 10 \text{ kHz}$ [37], $W^{ab} = 40\text{--}60 \text{ GHz}$ [30], and the density of dopants can be relatively large, $N \approx 10^{19} \text{ cm}^{-3}$. There is also a zero-phonon line at the $4d\text{--}5f$ electric-dipole allowed optical transition with the oscillator strength $f \sim 10^{-4}$ [30] and the wavelength $\lambda = 401\text{--}424 \text{ nm}$. According to Eq. (12), at the density of dopants $N = 10^{19} \text{ cm}^{-3}$, this should lead to $V_g \approx 10 \text{ m/s}$. The EIT threshold intensity would be $I_{thres} \approx 400 \text{ W/cm}^2$. In $\text{Eu}^{2+}:\text{MgS}$ the inhomogeneous width of the $f\text{--}d$ transition is rather large, $W^{ab} \sim 6 \text{ THz}$ [38], but the oscillator strength of the transition is $f \sim 0.01\text{--}0.02$ [38,39]. The wavelength of the $4f\text{--}5d$ transition is $\lambda = 578 \text{ nm}$ in this crystal. If we assume the width of the spin transition $W^{cb} \sim 10 \text{ kHz}$ and the density of dopant ions $N = 10^{19} \text{ cm}^{-3}$, this gives the group velocity estimate $V_g \approx 20 \text{ m/s}$. The intensity of the drive laser required for EIT to be observed would be $I_{thres} \approx 600 \text{ W/cm}^2$.

It is worth mentioning one more requirement in the proposed solid materials. It is desirable that in the Λ system under consideration both optical transitions be of comparable strength to avoid using high laser power. In principle, if the lower levels are different spin levels, both transitions to a common upper level cannot be allowed, since spin is conserved in optical transitions. This restriction can be overcome either by mixing of spin levels by an applied magnetic field [11] or by using atoms or ions with strong spin-orbit coupling in the case of electronic Zeeman lower levels, or strong spin-orbit and hyperfine interactions for hyperfine lower levels. These interactions lead to mixing of different electronic (nuclear) spin wave functions with spatial ones, thus making both optical transitions allowed. The rare-earth ions doped into dielectric crystals which we discuss above possess strong spin-orbit interaction because of their high atomic numbers, so transitions from Zeeman sublevels to a common upper level may be of equal strength [40]. In the case of hyperfine lower levels it is harder to find transitions with comparable strength, since the hyperfine interaction is small, and generally only transitions that preserve the nuclear spin I_z are allowed. However in hosts where a rare-earth ion occupies a site of low symmetry, nuclear state mixing by the crystal field can give rise to $\Delta I_z \neq 0$ transitions of comparable intensity [30,41].

So far, a large inhomogeneous broadening of the optical transition in solids has been viewed as a negative factor preventing the reduction of both EIT threshold intensity and group velocity. However, for certain applications a large inhomogeneous broadening can be helpful. Indeed, it has been widely used in developing optical memory based on the hole-burning technique [38]. It can be used also for quantum storage (storage of the quantum statistics and spatial-temporal form of optical pulses). This requires a combination of the recently suggested so called light storage technique [7] with the two-photon spin echo technique [26]. The latter is needed because of inhomogeneous broadening at the spin transition. This combined technique is the following. First, a weak signal pulse along with a strong and long (spatially uniform) driving pulse is inserted into a medium under EIT conditions. When it fully enters into the medium the driving field is switched off so that the signal pulse imprint is kept in the spatial distribution of the spin coherence. During a time interval t_0 shorter than the spin coherence decay time, the spins of different ions diverge until a microwave π pulse (or two simultaneous optical pulses resonant to $a \rightarrow b$ and $a \rightarrow c$ transitions) converts them back to produce the same total spin at the moment $2t_0$. (Note that populations of spin sublevels exchange after such a procedure. They can be switched back by applying another π pulse at the moment when the total spin is restored.) Sending a driving pulse into the medium at the moment when the total spin is restored would result in reproduction of the signal pulse. Recent experiments have successfully demonstrated this technique [26]. Note that its potential advantage in solid materials with $z < 1$ as compared to the light storage technique realized in gases [7,23] is the large number of information channels defined by the ratio of inhomogeneous to homogeneous line broadening. As in BEC experiments (but without involvement of the corresponding technical complications), it allows one to get rid of the smearing of information about the signal caused by atomic diffusion (taking place in gaseous cell experiments).

ACKNOWLEDGMENTS

The authors wish to thank DARPA, the Texas Advanced Technology and Research Program, and ONR for financial support.

APPENDIX

The mechanisms of inhomogeneous broadening at optical and hyperfine transitions in solids, caused by dipole-dipole and spin-spin interactions, respectively, are essentially different from each other. In particular, inhomogeneous broadening of hyperfine transitions typically is smaller than that of optical transitions, which is very favorable for the appearance of atomic interference effects. One has to average the susceptibility of a Λ system over the frequency distributions of one- and two-photon transitions independently:

$$\chi = \int d(\omega_{ab}) f(\omega_{ab}) \int d(\omega_{cb}) f(\omega_{cb}) \eta \left\{ \frac{\rho_{ab}}{\alpha} \right\}, \quad (\text{A1})$$

where ω_{ab} and ω_{cb} are the frequencies of the $a \rightarrow b$ and $c \rightarrow b$ transitions, $f(\omega_{ab(cb)})$ is the normalized frequency distribution function, ρ_{ab} is the coherence of the $a \rightarrow b$ transition induced by radiation fields, and $\eta = N\mu_{ab}^2/2\hbar$. The Rabi frequency of the probe field with frequency ν is defined by $\alpha = \mu_{ab}E_p/2\hbar$. The matrix element of the dipole moment between levels a and b is μ_{ab} , E is the probe field amplitude, and N is the atomic density.

For simplicity we model the frequency distribution with a Lorentzian function with full width at half maximum $2W^{ab(cb)}$ such that

$$f(\omega_{ab(cb)}) = \frac{W^{ab(cb)}/\pi}{(\Delta\omega_{ab(cb)})^2 + (W^{ab(cb)})^2}. \quad (\text{A2})$$

The susceptibility (A1) can now be evaluated by two contour integrations in the complex plane. Let us first integrate over $\Delta\omega_{ab}$. We choose the lower half plane, which contains two poles:

$$\Delta\omega_{ab} = -iW^{ab}, \quad -iy = -i\sqrt{\gamma^2 + \frac{\Omega^2\gamma(1+3w_{cb}/w_{ab})}{2w_{cb}}}.$$

So $\chi = \chi_1 + \chi_2$, where χ_i are the contributions from the two poles. For the pole $\Delta\omega_{ab} = -iW^{ab}$ we have

$$\chi_1 = \frac{i\eta}{2} \frac{(\gamma_{cb} + i\Delta + i\Delta\omega_{cb})[\gamma^2 + \gamma\Omega^2/w_{cb} + (iW^{ab} + \Delta\omega_{cb})^2] - \Omega^2(W^{ab} + \gamma - i\Delta\omega_{cb})}{[(W^{ab} + \gamma + i\Delta)(\gamma_{cb} + i\Delta + i\Delta\omega_{cb}) + \Omega^2][y^2 + (iW^{ab} + \Delta\omega_{cb})^2]}.$$

The second pole $\Delta\omega_{ab} = \Delta\omega_{cb} - iy$ yields

$$\chi_2 = -\frac{i\eta}{2} \frac{W^{ab} \left[\Omega^2(y + \gamma) - (\gamma_{cb} + i\Delta + i\Delta\omega_{cb}) \left(\gamma^2 - y^2 + \frac{\gamma\Omega^2}{w_{cb}} \right) \right]}{y[(W^{ab})^2 + (\Delta\omega_{cb} - iy)^2] \{ [y + \gamma + i(\Delta + \Delta\omega_{cb})](\gamma_{cb} + i\Delta + i\Delta\omega_{cb}) + \Omega^2 \}}.$$

Now we carry on an integration over $\Delta\omega_{cb}$, choosing again the lower half plane, since it contains fewer poles.

The χ_1 term contains the following poles in the lower half plane: $\Delta\omega_{cb} = -iW^{cb}$, $-i(W^{ab} + y)$, and $-i(W^{ab} - y)$. The last one lies in the lower plane only if $y < W^{ab}$. So there will be either two or three poles, depending on the value of y .

The χ_2 term multiplied by Eq. (A2) corresponding to the $c \rightarrow b$ transition contains the poles $\Delta\omega_{cb} = -iW^{cb}$ and $\Delta\omega_{cb} = -i(W^{ab} - y)$. Again, there are either two or one pole (s) in the lower half plane depending on whether y is greater or less than W^{ab} . It turns out that the contributions to χ_1 and χ_2 from the pole $\Delta\omega_{cb} = -i(W^{ab} - y)$ when $y < W^{ab}$ exactly cancel each other, so we are left with only three terms, χ_{11} and χ_{12} stemming from integration of χ_1 , and χ_{21} resulting from the integration of χ_2 , where

$$\chi_{11} = -\frac{i\eta}{2AZ_{11}} (B_{11} - \Delta^2 - i\Delta W^{ab})(C_{11} - i\Delta D_{11}),$$

$$A = y^2 - (W^{ab} - W^{cb})^2 \approx y^2 - (W^{ab})^2,$$

$$\begin{aligned} Z_{11} &= [(\gamma + W^{ab})(\gamma_{cb} + W^{cb}) + \Omega^2 - \Delta^2]^2 \\ &\quad + \Delta^2[\gamma + \gamma_{cb} + W^{ab} + W^{cb}]^2 \\ &\approx [W^{ab}W^{cb} + \Omega^2 - \Delta^2]^2 + \Delta^2(W^{ab})^2, \end{aligned}$$

$$B_{11} = (\gamma + W^{ab})(\gamma_{cb} + W^{cb}) + \Omega^2 \approx W^{ab}W^{cb} + \Omega^2,$$

$$\begin{aligned} C_{11} &= \Omega^2(\gamma + W^{ab} - W^{cb}) \\ &\quad + (\gamma_{cb} + W^{cb}) \left((W^{ab} - W^{cb})^2 - \gamma^2 - \frac{\gamma\Omega^2}{w_{cb}} \right) \\ &\approx \Omega^2W^{ab} + W^{cb}(W^{ab})^2 - \frac{\gamma\Omega^2}{w_{cb}}W^{cb}, \end{aligned}$$

$$D_{11} = \gamma^2 + \frac{\gamma\Omega^2}{w_{cb}} - (W^{ab} - W^{cb})^2 \approx \frac{\gamma\Omega^2}{w_{cb}} - (W^{ab})^2.$$

Here the following assumptions were used: $W^{ab} \gg \gamma, W^{cb}; W^{cb} \gg \gamma_{cb}$ and $w_{ab} \gg w_{cb}$. All of these inequalities typically hold for EIT experiments in solids.

The second term is

$$\begin{aligned} \chi_{12} &= -\frac{i\eta W^{cb}}{2y(y + W^{ab})^2 Z_{12}} [B_{12} - \Delta^2 - i\Delta(2W^{ab} + y)] \\ &\quad \times (C_{12} - i\Delta D_{12}), \end{aligned}$$

where

$$\begin{aligned} Z_{12} &= [(\gamma + W^{ab})(y + \gamma_{cb} + W^{ab}) + \Omega^2 - \Delta^2]^2 \\ &\quad + \Delta^2[\gamma + \gamma_{cb} + y + 2W^{ab}]^2 \\ &\approx [W^{ab}(y + W^{ab}) + \Omega^2 - \Delta^2]^2 + \Delta^2[y + 2W^{ab}]^2, \end{aligned}$$

$$\begin{aligned}
 B_{12} &= (\gamma + W^{ab})(y + \gamma_{cb} + W^{ab}) + \Omega^2 \\
 &\approx W^{ab}(y + W^{ab}) + \Omega^2, \\
 C_{12} &= \Omega^2(\gamma - y) - \frac{\gamma\Omega^2}{2w_{cb}} \left(1 - \frac{3w_{cb}}{w_{ab}}\right) (\gamma_{cb} + y + W^{ab}) \\
 &\approx \Omega^2(\gamma - y) - \frac{\gamma\Omega^2}{2w_{cb}} (y + W^{ab}), \\
 D_{12} &= \frac{\gamma\Omega^2}{2w_{cb}} \left(1 - \frac{3w_{cb}}{w_{ab}}\right) \approx \frac{\gamma\Omega^2}{2w_{cb}}.
 \end{aligned}$$

Finally,

$$\begin{aligned}
 \chi_{21} &= - \frac{i\eta W^{ab}}{2y[(W^{ab})^2 - (y + W^{cb})^2]Z_{21}} \\
 &\times [B_{21} - \Delta^2 - i\Delta(2W^{cb} + \gamma_{cb} + \gamma + y)] \\
 &\times (C_{21} - i\Delta D_{21}),
 \end{aligned}$$

where

$$\begin{aligned}
 Z_{21} &= [(\gamma + y + W^{cb})(\gamma_{cb} + W^{cb}) + \Omega^2 - \Delta^2]^2 \\
 &\quad + \Delta^2[\gamma + \gamma_{cb} + y + 2W^{cb}]^2 \\
 &\approx [(\gamma + y + W^{cb})W^{cb} + \Omega^2 - \Delta^2]^2 \\
 &\quad + \Delta^2[\gamma + y + 2W^{cb}]^2, \\
 B_{21} &= (\gamma + y + W^{cb})(\gamma_{cb} + W^{cb}) + \Omega^2 \\
 &\approx (\gamma + y + W^{cb})W^{cb} + \Omega^2, \\
 C_{21} &= \Omega^2(\gamma + y) - \frac{\gamma\Omega^2}{2w_{cb}} \left(1 - \frac{3w_{cb}}{w_{ab}}\right) (\gamma_{cb} + W^{cb}) \\
 &\approx \Omega^2(\gamma + y) - \frac{\gamma\Omega^2}{2w_{cb}} W^{cb}, \\
 D_{21} &= \frac{\gamma\Omega^2}{2w_{cb}} \left(1 - \frac{3w_{cb}}{w_{ab}}\right) \approx \frac{\gamma\Omega^2}{2w_{cb}}.
 \end{aligned}$$

-
- [1] S.E. Harris, Phys. Today **50**, 36 (1997).
 [2] E. Arimondo, Prog. Opt. **35**, 259 (1996).
 [3] J.P. Marangos, J. Mod. Opt. **45**, 471 (1998).
 [4] S.E. Harris, and L.V. Hau, Phys. Rev. Lett. **82**, 4611 (1999).
 [5] M.D. Lukin, and A. Imamoglu, Phys. Rev. Lett. **84**, 1419 (2000).
 [6] O. Kocharovskaya, Y. Rostovtsev, and M.O. Scully, Phys. Rev. Lett. **86**, 628 (2001).
 [7] M. Fleischhauer and M.D. Lukin, Phys. Rev. Lett. **84**, 5094 (2000).
 [8] B.S. Ham, P.R. Hemmer, and M.S. Shahriar, Opt. Commun. **144**, 227 (1997).
 [9] C. Wei and N.B. Manson, Phys. Rev. A **60**, 2540 (1999).
 [10] C. Wei and N.B. Manson, J. Opt. B: Quantum Semiclassical Opt. **1**, 464 (1999).
 [11] P.R. Hemmer, A. Turukhin, M.S. Shahriar, and J. Musser, Opt. Lett. **26**, 361 (2001).
 [12] H. Schmidt *et al.*, Laser Phys. **9**, 797 (1999).
 [13] H. Schmidt, K.L. Campman, A.C. Gossard, and A. Imamoglu, Appl. Phys. Lett. **70**, 3455 (1997).
 [14] M.M. Kash, V.A. Sautenkov, A.S. Zibrov, L. Hollberg, G.R. Welch, M.D. Lukin, Y. Rostovtsev, E.S. Fry, and M.O. Scully, Phys. Rev. Lett. **82**, 5229 (1999).
 [15] G.R. Welch *et al.*, Found. Phys. **28**, 621 (1998).
 [16] A. Javan, O. Kocharovskaya, H. Lee, and M.O. Scully, Phys. Rev. A **66**, 013805 (2002).
 [17] K.-J. Boller, A. Imamoglu, and S.E. Harris, Phys. Rev. Lett. **66**, 2593 (1991).
 [18] M.S. Feld and A. Javan, Phys. Rev. **177**, 540 (1969).
 [19] A.V. Taichenachev, A.M. Tumakin, and V.I. Yudin, JETP Lett. **72**, 119 (2000).
 [20] A. S. Zibrov (private communications).
 [21] M.D. Lukin, M. Fleischhauer, A.S. Zibrov, H.G. Robinson, V.L. Velichansky, L. Hollberg, and M.O. Scully, Phys. Rev. Lett. **79**, 2959 (1997).
 [22] S.E. Harris, J.E. Field, and A. Kasapi, Phys. Rev. A **46**, R29 (1992).
 [23] L.V. Hau, S.E. Harris, Z. Dutton, and C.H. Behroozi, Nature (London) **397**, 594 (1999).
 [24] A. Kasapi, M. Jain, G.Y. Yin, and S.E. Harris, Phys. Rev. Lett. **74**, 2447 (1995).
 [25] D. Budker, D.F. Kimball, S.M. Rochester, and V.V. Yashchuk, Phys. Rev. Lett. **83**, 1767 (1999).
 [26] A.V. Turukhin, V.S. Sudarshanam, M.S. Shahriar, J.A. Musser, B.S. Ham, and P.R. Hemmer, Phys. Rev. Lett. **88**, 023602 (2002).
 [27] P.A. Tanner, C.S.K. Mak, and M.D. Faucher, Chem. Phys. Lett. **343**, 309 (2001).
 [28] D. Pehler, and N. Edelstein, Phys. Rev. A **41**, 6406 (1990).
 [29] D. Van Der Voort, and G. Blasse, J. Solid State Chem. **87**, 350 (1990).
 [30] D.M. Boye, R.M. Macfarlane, Y. Sun, and R.S. Meltzer, Phys. Rev. B **54**, 6263 (1996).
 [31] S. Lizzo, A.H. Velders, A. Meijerink, G.J. Dirksen, and G. Blasse, J. Lumin. **65**, 303 (1996).
 [32] T. Hoshina and S. Kuboniwa, J. Phys. Soc. Jpn. **31**, 828 (1971).
 [33] G.J. Pryde, M.J. Sellars, and N.B. Manson, Phys. Rev. Lett. **84**, 1152 (2000).
 [34] I.T. Jacobs, G.D. Jones, K. Zdansky, and R.A. Satten, Phys. Rev. B **3**, 2888 (1971).
 [35] M.H. Crozier, Phys. Rev. **137**, A1781 (1965).
 [36] T. Yosida, M. Yamaga, D. Lee, T.P.J. Han, H.G. Gallagher, and B. Henderson, J. Phys.: Condens. Matter **9**, 3733 (1997).
 [37] J.M. Baker, and F.I.B. Williams, Proc. R. Soc. London, Ser. A **257**, 283 (1962).
 [38] L. Biyikli, and Z. Hasan, J. Lumin. **83/84**, 373 (1999).
 [39] Z. Hasan, L. Biyikli, and P.I. Macfarlane, Appl. Phys. Lett. **72**, 3399 (1998).
 [40] R.M. Macfarlane, and J.C. Vial, Phys. Rev. B **36**, 3511 (1987).
 [41] L.E. Erickson, Phys. Rev. B **16**, 4731 (1977).